

DIAGNOSTIC TOOLS FOR THE UNDUATOR SYSTEM OF THE SEEDED HGHG-FEL AT MAX-LAB

J. Bahr[#], M. Abo-Bakr, W. Frentrup, A. Gaupp, K. Holldack, M. Scheer,
BESSY, Berlin, Germany

J. Kuhn[#], S.K. Höffgen, U. Weinand, Fraunhofer INT, Euskirchen, Germany
S. Werin, S. Thorin, F. Lindau, MAX-lab, Lund, Sweden

Abstract

Within a collaboration between MAX-lab and BESSY a one stage seeded HGHG-FEL has been set up at Max-lab. BESSY has built the undulator system consisting of a modulator, a radiator and an electromagnetic chicane. BESSY has also installed three types of diagnostic tools: optical fibres for a fast Cherenkov beam loss detection, optical fibres for absolute dose measurements via their radiation-induced attenuation and THz detectors for the characterization of electron bunch properties. During first injections with a laser driven rf-gun the Cherenkov fibres have delivered detailed spatial information on the beam losses inside the beamline. Over the last year the second system, based on powermeter measurements, has detected a total dose of 180Gy. The high sensitivity and low drift of this system has been demonstrated. A THz detector behind the last dipole magnet close to the beam dump provides information on the bunch compression and the laser induced energy modulation. We report on the measurements performed with these diagnostics tools.

INTRODUCTION

Over the last years MAX-lab and BESSY have set up a one stage seeded HGHG-FEL [1] at MAX-lab. The FEL will be seeded with a 266nm Ti:Sa laser and it will radiate on the third and fifth harmonic at 89nm and 53nm. This device will be used for studying the HGHG-FEL process comparing FEL simulations with measurements and for the development and testing of FEL relevant equipment.

The general layout of the system has been described in [2]. Detailed GENESIS simulations are presented in [3-4]. The undulator and chicane parameters are documented in [5-6]. For the FEL experiment the existing BaO cathode of the thermionic gun and a 266nm Ti:Sa laser are used as an rf gun producing bunches with a length of 10ps. The bunches are accelerated in the MAX-lab recirculator to 400MeV and compressed in the recirculator and the dogleg down to 30fs. The peak current, the emittance and the energy spread just before entering the modulator are 1.3kA, 4mm mrad and 0.25%, respectively.

After the transport of the undulators from BESSY to MAX-lab the field integrals have been measured at the final location in the horizontal orientation using a pulsed wire system. Before shipping the magnetic measurements have been done at the BESSY measurement bench in the

vertical orientation. Based on the pulsed wire measurements the residual field integrals have been compensated with horizontal and vertical air coils at either end of each undulator.

CHERENKOV FIBERS

Electron beam losses produce Cherenkov radiation in silica fibres which can be used as a fast diagnostic tool during first alignment [7]. First commissioning of the set up has been done with the thermionic gun which produces 200ns bunch trains. The fibre system shows a convolution of the longitudinal bunch train profile and the distribution of electron losses which can hardly be disentangled (figure 1). Nevertheless, the total losses give some information on the electron beam alignment. The bunches as produced by the rf-gun have a length in the sub-ps regime and they are well suited for the detection of hot spots of electron losses. Without any screen moved into the beam two peaks show up (figure 1). They correspond to the horizontal aperture at the seed laser dogleg and the circular aperture of the modulator vacuum chamber. By minimizing these two peaks the electron beam position can be aligned.

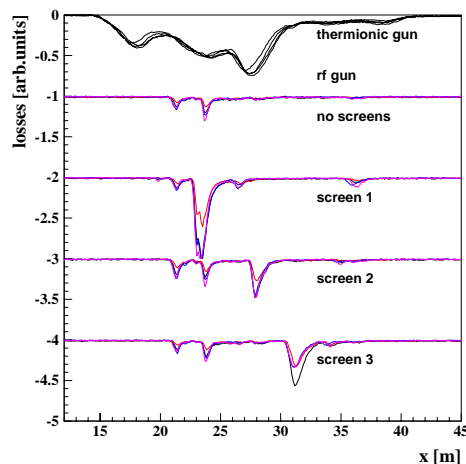


Figure 1: Electron losses along the undulator beamline as measured with four Cherenkov fibres. Black: thermionic gun, coloured: rf gun. The screens are located: 1) in front of the modulator, 2) in front of the chicane, 3) in front of the radiator.

Normalized differences of the four Cherenkov fibre signals provide spatially resolved information on the losses in the four quadrants [7]. The sensitivity of such a system can be explored by means of GEANT simulations

[#] corresponding author:
Johannes.Bahr[#]@bessy.de

[8]. Generally, an electron hitting the vacuum chamber produces Cherenkov radiation in all four fibres. The quality of the spatial information depends on the achievable asymmetry of the signals. We studied the extreme cases where the electrons hit the circular beam pipe of the modulator at the upstream flange with azimuthal angles of 0° , 45° and 90° . The fibres are located at azimuthal angles of 45° , 135° , 225° and 315° . The highest signal and the largest asymmetry are found for the 45° case. For the 0° and 90° case the asymmetries are weaker but still pronounced (figure 2). Based on the results summarized in table 1 an absolute value for the spatial resolution of the electron beam position can be extracted if the electron beam density distribution close to the vacuum chamber is known. In a next step the electron phase space as simulated with GENESIS will be used for this purpose. Currently, the Cherenkov control system is modified such that the preprocessed information will be available in EPICS format during commissioning.

The smaller line width of the calculated structures as compared to the measured peaks is partly due to the resolution of measurement system.

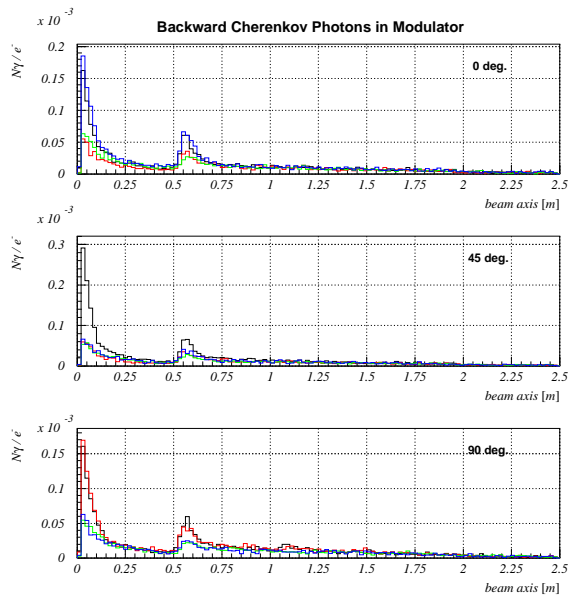


Figure 2: Number of Cherenkov photons in backward direction per electron hitting the upstream flange of the modulator chamber. The first peak corresponds to the losses at the entrance of the beam pipe whereas the second peak indicates losses at the upstream end of the modulator structure.

Table 1: Total number of Cherenkov photons per electron for loss angles of 0° , 45° and 90° .

Fibre position	0° losses	45° losses	90° losses
45°	0.00255	0.00341	0.00277
135°	0.00171	0.00186	0.00286
225°	0.00194	0.00189	0.00193
315°	0.00285	0.00206	0.00191

POWERMETER SYSTEM

Radiation sensitive P-doped graded-index optical fibres have proven to be useful monitors to measure absolute doses deposited in a beamline [9]. Powermeter systems have been installed at FLASH [10], DELTA [11] and, recently, at MAX-lab [6]. In [6] the fibre characteristics are described in detail. 15 sensors are distributed along the undulator system and one channel is used as a reference. The MAX-lab system has taken data now for one year (figure 3).

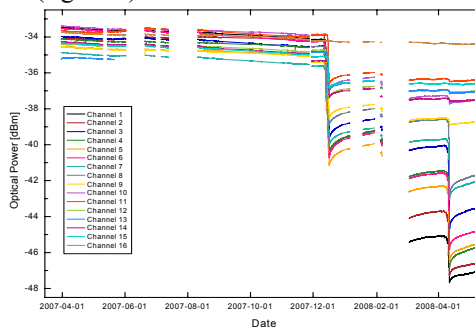


Figure 3: Raw data measured over one year. The sensors are located inside the modulator and radiator upstream (us) and downstream (ds) of the center. Sensors: 1-4: modulator-us, 5-8: modulator-ds, 9-12: radiator-us, 13-15: radiator-ds, sensor 16: reference channel.

The raw data have been processed as follows:

- i) Detecting of significant signal changes by comparing to an averaged value (A) which is calculated by $A_{new} = (A_{old} \cdot (N-1) + V) / N$ with V = non averaged data, N = number of data points for averaging (typically 3).
- ii) Correction for light source fluctuations.
- iii) Correction for the annealing process of colour centres after irradiation.
- iv) Calibration based on measurements with a Co-60 source before installation (figure 4).

The system shows a low drift of only 3 Gy per year which is significantly lower than the value of up to 1 Gy per week as estimated for FLASH. This is mainly due to the high stability of the light source and an extremely stable light distribution system. Another improvement of the MAX-lab system is the reduction of data acquisition time for 16 channels from 7 to currently 2 minutes which permits a more detailed analysis of beam losses during commissioning. Depending on the averaging times chosen the response time can be reduced even to 1 minute with slightly higher noise. Furthermore, the light source can now be operated remotely via an USB port which enables a remote control of the complete system from BESSY in Berlin. All data are transferred automatically via internet to BESSY and the Fraunhofer INT for further analysis.

During first alignment of the electron beam in the undulator system a thermionic gun has been used. The charge of a bunch train generated with this gun was approximately 1nC and the repetition rate was 0.5Hz. After one year of operation the undulators have seen doses of up to 180Gy. Generally, the doses were significantly lower with the rf gun (0.07nC, 2Hz repetition rate) than with the thermionic gun. As expected

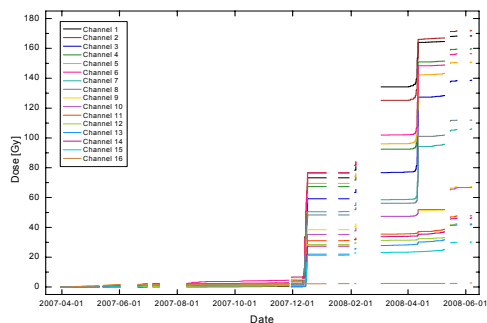


Figure 4: Calibrated data taken over a period of one year. The accumulated noise in the reference channel amounts to 3 Gy which is below 2% of the maximum dose.

the doses are higher at the upstream end of the modules and decrease over the length of the undulator modules. A blow up of the data demonstrates the high spatial resolution of the system (figure 5). A modification of the beam parameters is clearly visible in the different response of the individual sensors. After steering the electron beam (at 1:50pm) the sensors 7 and 8 show significantly higher doses than the sensors 5 and 6 whereas for earlier times all four sensors indicate similar doses.

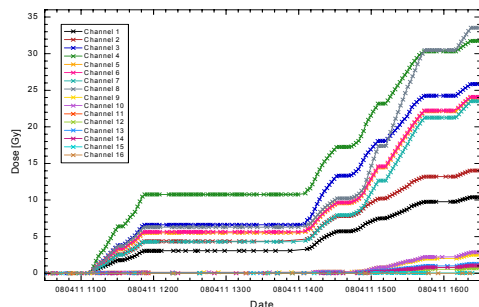


Figure 5: This graph demonstrates the high spatial resolution of the powermeter system.

THZ-RADIATION

In order to follow the track of a possible independent seed diagnostics using coherent synchrotron radiation (CSR) [6,12] a compact THz port was added to the dump magnet in order to extract CSR after the FEL interaction and the radiator. The setup is depicted in figure 6.

Calculating the SR angular pattern after the dump magnet in the FIR for 1 T at 1.3 m radius (critical energy 106 eV) one finds that the natural opening angle at 10 THz is ~ 40 mrad and ~ 80 mrad at 1 THz. Hence, SR (including edge radiation) can be extracted from both sides of the electron beam after a bend, which makes a THz “beamline” very compact (it fits into a UHV-CF35 T-piece). In the present case, the two 90° reflecting Al mirrors are located only 400 mm after the center of the bend accepting 50 mrad horizontally and 35 mrad vertically as limited by the 10 mm height of the vacuum chamber. The electron beam passes through a 10 mm wide slit between the mirrors. After being transmitted through a 2 mm thick quartz window, the THz pulses are detected either by a broad band pyroelectric crystal

(Deuterated Triglycine Sulphate, DTGS) [13] or by an InSb hot-electron-bolometer [14] of 1 THz bandwidth and 10^4 V/W sensitivity.

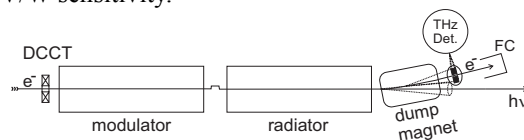


Figure 6: Setup for the THz diagnostics on the dump magnet at the MAX-lab test-FEL. The electron beam, after being deflected, passes through the middle of two Al-mirrors (~ 200 mm behind the bend) and is then focused onto the detector by a 90° deflecting off-axis paraboloid of 180 mm focal length. Bunch charge information is available from a current transformer (DCCT) and a Faraday cup (FC) acting as beam dump.

Results

After realizing that the pyroelectric detector has a lack of dynamic range at the bunch charges available (< 50 nC on crest), the InSb bolometer (featuring 108 h LHe hold time) could be driven to saturation (6 V) by one single THz pulse. The THz signal dependence on the bunch charge (detuning a solenoid after the gun) at a rep-rate of 2 Hz is depicted in figure 7 (left). The noise arises from fluctuations of the bunch charge as also indicated by losses along the structure. The signal increases nonlinearly with the number of electrons per pulse, as expected for CSR. There are deviations from a pure square dependency, most likely given by a charge dependent bunch shape.

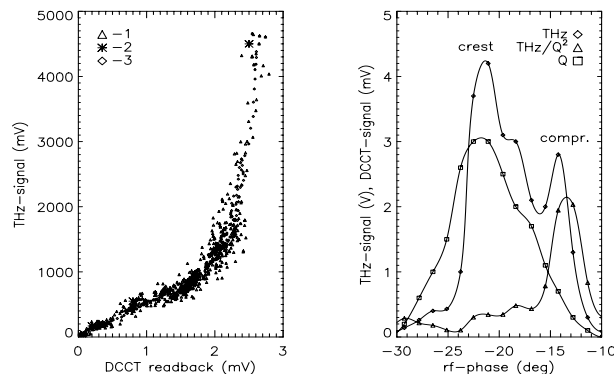


Figure 7: THz-signal from the InSb-detector (THz) during changes of the bunch current (left, 3 different records) and during a sweep of the rf-phase from -30 to -10 deg (right). The DCCT-signal being proportional to the bunch charge (Q) was used to determine the THz signal normalized to the square of the bunch charge (THz/Q^2).

The signal (5 shot average) was then acquired during scans of the rf-phase starting from -30° . A maximum in the bunch charge is always found at the nominal crest value of -22° , the THz maximum is slightly shifted to lower absolute values. Obviously, there is already significant CSR without compression indicating ps bunches. Moving off crest towards lower absolute values, a pronounced 2nd maximum was observed 8° away from the crest maximum, while the charge gradually decreases.

In order to correct for that, the square-normalized THz signal was plotted showing a shifted maximum at 8.4° off-crest.

Simulation

To simulate the current and compression curves we calculate the bolometer signal P_{tot} according to: (1)

$$P_{tot} = \int_0^{\infty} L(\omega)p(\omega) [N + N(N-1)|F(\omega)|^2]H(\omega)d\omega \quad (1)$$

where p is the SR emitted by a single electron, F is the magnitude of the Fourier-transform of the longitudinal particle distribution in the bunch, N is the number of electrons in the bunch and $L(\omega)$ and $H(\omega)$ are the low and high pass transmission functions of the setup including vacuum chamber (L) and detector and window (H). Calculating a low frequency cut-off by shielding $L=(h/R)^{-1/2}/2h=5.7 \text{ cm}^{-1}$ [15], where h is the 10 mm height of the dipole chamber and $R=1.3 \text{ m}$ is the bend radius, using the measured -3db cut-off value of the InSb detector of $H = 30 \text{ cm}^{-1}$ and further normalizing to N^2 at $N \gg 1$ we find:

$$P_{tot} / N^2 \approx \int_L^H p(\omega) |F(\omega)|^2 d\omega \quad (2)$$

For F we use the Fourier transform of the longitudinal current profiles assuming a Gaussian shape for simplicity.

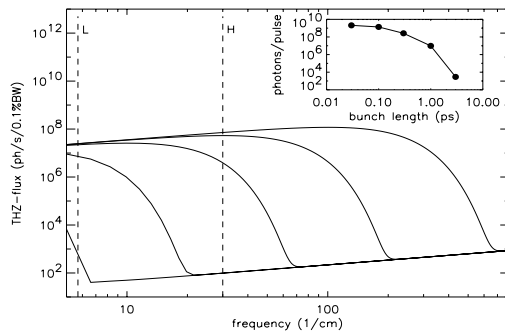


Figure 8: Expected CSR spectra (Gaussian bunch model) from the dump magnet at 50 pC bunch charge and 2 Hz repetition rate for 3, 1, 0.3, 0.1, 0.03 ps (from left to right). The inset shows the total No. of photons/pulse vs. rms-bunch length from the InSb-bolometer integrating between L and H.

The InSb-bolometer accepts only a limited bandwidth as depicted in figure 8. The total number of photons/pulse becomes gradually less sensitive to short bunch lengths but still increases. Hence, a maximum bunch compression means maximum THz power despite bandwidth limited detection. A semi-quantitative analysis depicted in figure 9 compares the measurements to the simple model described above. A linear compression and decompression along the phase difference from crest was assumed. Starting from 1 ps rms bunch length, a very sensitive response on the compression ratio is available from the width of the compression scan and from the background THz signal on crest. Maximum THz signal at minimum width indicates sub-ps compression. Since the seed in

combination with R_{56} in the dump magnet is expected to cause significant bunch lengthening [6] a seed diagnostics is planned for the next run in combination with a bunch length detection measuring the THz spectra.

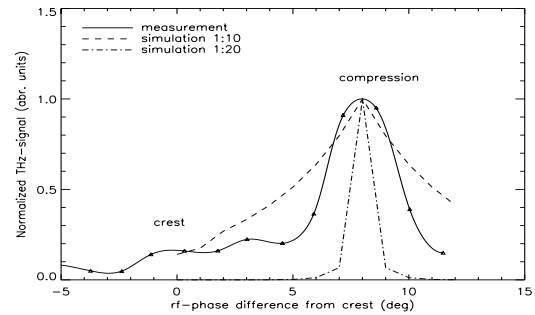


Figure 9: Comparison of the measured THz-signal during the rf-phase scan with simulations according to the model.

Detecting the CSR from the dump magnet is a valuable tool to tune up the bunch compression. Employing bolometers, there is sufficient dynamic range to detect THz signals from bunch charges $< 0.1 \text{ pC}$. Planned measurements of the THz spectra and THz-laser cross correlation promises much more diagnostic information on energy modulation and temporal stability, both being indispensable prerequisites of a successful lasing in the VUV.

REFERENCES

- [1] L. H. Yu, J. Wu, Nucl. Instr. and Meth. in Nucl. Res. A 483 (2002) 493.
- [2] M. Brandin et al., Proceedings of the FEL 2007, Novosibirsk, Russia, 2007, pp 513-516.
- [3] S. Thorin, Phys. Rev. ST Accel. Beams, 10, 110701-1-5 (2007).
- [4] S. Thorin et al, Proceedings of the EPAC, Genoa, Italy, 2008, to be published.
- [5] J. Bahrtd et al., Proceedings of the EPAC, Edinburgh, Scotland, 2006, pp 59-61.
- [6] J. Bahrtd et al., Proceedings of the FEL Conference, Novosibirsk, Russia, 2007, pp 122-125.
- [7] M. Körfer, W. Göttmann, F. Wulf, J. Kuhnenn, Proc. of DIPAC 2005, Lyon, France, 2005, p. 301.
- [8] GEANT 3.21, Detector Description and Simulation Tool, Computing and Networks Division, CERN, Geneva, Switzerland.
- [9] H. Henschel, M. Körfer, J. Kuhnenn, U. Weinand, F. Wulf, Nucl. Instr. and Meth. in Phys. Res. A 526 (2004) pp. 537-550.
- [10] H. Henschel et al., Proceedings of DIPAC 2003, Mainz, Germany, pp 248-250.
- [11] Proceedings of the 2008 EPAC, Genoa, Italy, 2008.
- [12] K. Holldack, A.A. Zholents, Proc. FEL 2006, Berlin, Germany, p. 725, <http://www.JACoW.org>.
- [13] Bruker Optics, Ettlingen, Germany.
- [14] QMC Ltd., <http://www.thz.co.uk>.
- [15] J.S. Nodvick, D. Saxon, Phys. Rev. 96, B190 (1954).